Published in final edited form as:
Mech Dev. 2007 January ; 124(1): 35–42.

Tbx16 cooperates with Wnt11 in assembling the zebrafish organizer

Jonathan B. Muyskens and **Charles B. Kimmel**
Institute of Neuroscience, 1254 University of Oregon, Eugene, OR 97403-1254

Abstract

The organizer, the signaling center that specifies vertebrate axial polarity and the nervous system, is a dorsal midline mesodermal domain in the gastrula that will form prechordal plate and anterior notochord. We show that in zebrafish the organizer is not a single domain when it first arises in the nascent mesoderm at the onset of gastrulation. Rather, in the presumptive prechordal plate region, the organizer is subdivided into two side-by-side cellular fields. Within minutes, concurrent medial and anterior cellular movements merge, or 'coalesce', the two fields to form the well-known singular midline field. Coalescence forms a symmetrical domain because the cell movements on the left and right sides initiate simultaneously, and occur synchronously. However in embryos with reduced function of the T-box transcription factor Tbx16 (Spadetail), or its genetic target Paraxial protocadherin (Papc), synchrony is lost, coalesence is disrupted, and the midline domain is misshaped. Furthermore, with combined loss of Tbx16 and Wnt11 (Silberblick), coalesence is essentially absent. Possibly as a consequence, both the anterior movement of presumptive prechordal plate and organizer function, as assayed by eye-field separation, are disrupted. Our findings thus reveal that Tbx16, in combination with Wnt11, are critical components not only in morphogenesis but also in initial assembly of the organizer.

Keywords

gastrulation; T-box transcription factors; planar cell polarity

Introduction

Germ layer development in a vertebrate occurs during gastrulation, with cells that will form endoderm and mesoderm segregating internally to prospective ectoderm to occupy deep regions of the embryo. Among the first cells to internalize are dorsal midline cells of the organizer, a critical region discovered in classical grafting experiments to specify embryonic polarity and dorsal tissue fates, including the central nervous system (Spemann, 1924) and which we now understand to function by releasing extracellular signaling molecules including BMP antagonists (Solnica-Krezel, 2005). Organizer activity is focused in cells that will develop a transient axial head mesodermal domain, the prechordal plate. Therefore, characterizing prechordal plate morphogenesis and formation, and their control, provides essential background for understanding the global patterning of the embryo.

Corresponding Author: Jonathan Muyskens E-mail: muyskens@uoneuro.uoregon.edu, Telephone: 541-346-4506, Fax: 541-346-4548..

Results and Discussion

Presumptive Prechordal Plate Formation Involves Coalescence of Two Apposed Domains

In the zebrafish, the presumptive prechordal plate internalizes at the dorsal margin of the blastoderm prior to the formation of a structure called the shield, a thickening of cells on the dorsal aspect of the embryo that represents one of the first overt signs of gastrulation (Kimmel et al., 1995). We observed that the presumptive prechordal plate forms not from a single domain of cells at the midline, as previously had been assumed, but from two domains (Fig. 1). Early expression of the prechordal plate marker *gsc* was frequently manifested as two apposed, oblong marginal domains (Fig. 1B). Examining the live embryo with Nomarski DIC optics, we observed a demarcation, or boundary, approximately at the midline, where cells of the left and right side of the presumptive prechordal plate lined up in apposition. The demarcation (arrowhead, Fig. 1C) persisted for approximately 5 minutes after which the internalized field of cells appeared uniform. To characterize the cellular rearrangements during this period, we fluorescently labelled cell membranes and made time-lapse recordings with which we could track movements of presumptive prechordal plate cells in 3 dimensions (Fig. 1D–F, and Movie 1 in Supporting Information). Newly internalized cells make two separate inward bulges into underlying yolk syncytial layer (Fig. 1D). The cells transiently line up at the midline to form the demarcation (Fig. 1E), which is then erased by medial and anterior cell movement (Fig. 1E, F). Therefore, assembly of the zebrafish organizer involves the merging of two side by side populations of presumptive prechordal plate cells into one domain just following the onset of gastrulation. We refer to the merging process as coalescence.

Tbx16 is required for synchronous anterior and medial movement across the dorsal midline

How is the process of coalescence regulated? We find that in embryos with severe loss of function of the T-box transcription factor Tbx16 (Spadetail), morphogenesis accompanying coalescence is highly abnormal. A role of Tbx16 in prechordal plate morphogenesis has not been reported until now, however previous work has shown that *tbx16* is expressed in presumptive prechordal plate cells beginning in the blastula, and that its function is required in the late blastula for dorsal cells (putative prechordal plate and notochord precursors) to undergo compaction and acquire extensive cell-to-cell contacts (Warga and Nusslein-Volhard, 1998).

Complementing these reports, we observe that *tbx16* mutants, or embryos injected with a *tbx16* morpholino (MO), frequently displayed prominent asymmetry of the newly internalized prechordal plate. In time-lapse recordings, the wild-type presumptive prechordal plate shows mirror-image symmetry across the midline, before (Fig. 2A, Movie 2), during, and after (Fig. 2C) coalescence. In contrast, Fig.s 2B and D (Movie 3) are from a recording of a *tbx16* mutant in which the left side of the presumptive prechordal plate is several cell diameters broader than the right side. The same defect is apparent in embryos in which the presumptive prechordal plate is specifically labeled with a *gsc*-GFP transgene; we observe a symmetric prechordal plate domain soon after internalization in the wild type (Fig. 2E), and an asymmetric one in the *tbx16* mutant or *tbx16* MO-treated embryo (Fig. 2F). In the example shown, the more anteriorly positioned field of labelling is on the right side, in contrast to the case in Fig. 2C where it is on the left. We did not observe any consistent left or right sidedness to the aberrant expression pattern. Because we observe asymmetry in the null *tbx16* mutant (which of course lacks functional Tbx16 in all cells), the asymmetry phenotype cannot be accounted for simply by heterogenous knockdown of function, which might possibly occur in morphants.

The more anteriorly-positioned side of the asymmetrical domain was consistently larger than the opposite, more posterior one, suggesting that the initiation of anteriorly-directed movements of the internalized presumptive prechordal plate cells occur asynchronously on the

two sides. We tracked individual cells through the period of coalescence to examine this possibility directly. We observed that normally, following internalization, nearly all presumptive prechordal plate cells exhibit directional medial and anterior movement (Fig. 2G; such directed tracks color-coded blue for clarity of presentation). In the *tbx16* MO-treated embryo shown in Fig. 2H, the left side of the presumptive prechordal plate initiated anterior movement before the right. On the left (advanced) side, most of the cell movements were directional, comparable to the uninjected control. Strikingly, only a fraction of the cells on the right (delayed) side exhibited the same behaviour. Aberrantly moving cells (color-coded red) meandered non-directionally during at least the early part of the recording. Some of these aberrant cells recovered directional anterior movement during the recording period, others did not. Thus, we conclude that Tbx16 function is required for the synchronous initiation of coherent, directional cell movement on the two sides of the presumptive prechordal plate during coalescence. We note that synchronous movement does not necessarily imply that the left and right sides communicate with one another. Instead, with the presence of Tbx16 function, the movements could simply be regulated with high fidelity, making the timing of coalescence very precise.

Papc Mediates the Regulatory Function of Tbx16 in Presumptive Prechordal Plate Morphogenesis

Failure of coherent directed movement might be due to loss of adhesive contacts (Gumbiner, 2005) and/or signaling interactions among prechordal plate cells, and a candidate that could mediate both functions is Paraxial protocadherin (Papc), a genetic target of *tbx16* (Yamamoto et al., 1998) and a homophilic adhesion molecule (Kim et al., 1998). In *Xenopus laevis*, Xpapc is necessary for polarized movements of explanted mesodermal cells, and signals through RhoA to mediate separation behaviour in explanted tissue (Medina et al., 2004; Unterseher et al., 2004). Mutations in *papc* are unavailable, and to carry out loss-of-function analyses we used a dominant negative construct (*dn-papc*) that lacks both transmembrane and intracellular domains and thus forms a secreted peptide (Yamamoto et al., 1998). In a subset of embryos injected with a low dose of *dn-papc*, *gsc* expression in the early gastrula was both closer to the margin than in controls and the expression domain was asymmetrically shaped, phenocopying the defect described above with loss of Tbx16 (Fig. 3A, B). Reducing Papc function more severely, with a higher dose of *dn-papc* causes substantially more severe mispatterning of *gsc* expression, in fact the reduction is more substantial than when Tbx16 function itself is eliminated (quantification in Supporting Fig. 1). These findings show that Papc is necessary for proper cell movements of the presumptive prechordal plate, but do not explain why movement is asynchronous with loss of Tbx16. Furthermore, it is unclear why the loss of Papc phenotype is more severe than loss of Tbx16, because previous work demonstrated that *papc* expression and function requires Tbx16 during gastrulation (Yamamoto et al., 1998). Neither partial function nor maternal contribution of Tbx16 can resolve this issue because we used a null allele of *tbx16* and *tbx16* mRNA is not maternally supplied (Griffin et al., 1998). However, because Lim family transcription factors initiate *papc* expression in mouse and frog, (Hukriede et al., 2003) we considered the possibility that *papc* expression might be initiated independently of Tbx16, by examining *papc* expression in the *tbx16* mutant.

In agreement with Yamamoto et al. (1998), we find that Tbx16 is required for *papc* expression following the onset of gastrulation (data not shown). However, at the time of earliest expression in the late blastula, *papc* expression was indistinguishable among embryos derived from a clutch of heterozygous *tbx16* parents, among which 1/4 are expected to be mutant (data not shown). Therefore, a factor in addition to Tbx16 must be prominently involved in the initiation of *papc* expression. Within ten minutes of the expression of the earliest transcripts (about 15 minutes before internalization begins), 76% of the embryos (38/50) strongly expressed *papc* around the margin (Fig. 3C), whereas 24% of the embryos (12/50), the putative *tbx16*

homozygotes, displayed weak, patchy expression, that frequently was asymmetric, stronger on one side of the midline than the other (Fig. 3D). The level of *gsc* expression was not reduced in *tbx16* mutants at this stage (data not shown), arguing that the loss of *papc* expression was not due to cell loss, but to misregulation of transcription.

Hence early expression defects of *papc* correlate with, and we propose, cause incoherent, nonuniform cell movement and disrupted coalescence in *tbx16* mutants. This hypothesis predicts that following internalization, in *tbx16* mutants in which anterior movement is asymmetric, we should observe *papc* expression to be asymmetric as well, with the side showing higher *papc* expression consistently advanced farther anteriorly than the side with low *papc* expression. We tested this prediction by examining *papc* expression in embryos about 35 minutes after the onset of presumptive prechordal plate internalization. Expression in *tbx16* mutants at this stage is patchy and substantially reduced in comparison to wild type (Fig. 3D, E, 24/98 embryos from a clutch of *tbx16* heterozygous parents displayed reduced *papc* expression). Supporting our hypothesis, in mutants where expression of *papc* is substantially greater on one side of the dorsal margin than the other, the side with greater expression was advanced farther anteriorly than the cells on the weakly expressing side (n=8/24; 16/24 mutants did not have a recognizable left-right bias in expression, consistent with our earlier observation that not all *tbx16* mutants display asymmetric emergence of the presumptive prechordal plate). We did not observe embryos displaying the converse phenotype, greater anterior displacement on the side with weak *papc* expression (n=0/24). Thus, we argue that Tbx16 plays a critical function in the coherent initiation of directed anterior and medial movement of presumptive prechordal plate cells by regulation of full expression of *papc*.

Loss of Both Tbx16 and Wnt11 Blocks Coalescence Nearly Completely and Disrupts Organizer Function

Whereas loss of Tbx16 substantially disturbs early morphogenesis of the presumptive prechordal plate, coalesence nevertheless occurs, albeit abnormally. Following the onset of gastrulation, the prechordal plate domain advances anteriorly more slowly than in wild-type embryos, and is broader, as judged by expression of *gsc* (Fig. 4A, B; quantified in Supporting Fig. 1). The expression domain often remained asymmetrically shaped at this stage in *tbx16* MO-treated embryos. In addition, we observe that *gsc* is downregulated in posterior prechordal plate cells in *tbx16*$^{-}$ embryos and *tbx16*-MO embryos, similar to what has been reported for *pitx2c* expression at mid-gastrulation (Essner et al., 2000). By the end of gastrulation, morphogenesis has apparently regulated, for we were not able to detect any difference in the position or shape of the *gsc* expression domain between wild types and *tbx16* mutants (Fig. 4E, F). After another twelve hours of development when the primary organs have formed, eye field separation, a read-out of proper prechordal plate movement (Ulrich et al., 2003), appeared normal (Fig. 4I, J; quantified in Supporting Fig. 2).

Another protein, Wnt11 (Silberblick), is known to play a critical signalling function during prechordal plate morphogenesis (Ulrich et al., 2003; Ulrich et al., 2005). Surprisingly, we observed no defect in coalescence in *wnt11* mutants or MO-treated embryos, even though presumptive prechordal plate cells lacking Wnt11 move more slowly and are less directed than in the wild-type (Ulrich et al., 2003), as we confirm for the early gastrula. In particular, we observe that in *wnt11* mutants the *gsc* expression domain is broad and nearer the margin than in wild-type or *tbx16* MO-treated embryos (Fig. 4C). Unlike the *tbx16* mutant, we do not observe recovery by the end of gastrulation in the *wnt11* mutant. Instead, the prechordal plate remains short and wide relative to wild type (Fig. 4G), as previously described (Heisenberg et al., 2000). In the 1-day embryo the eyes are not well separated (Fig. 4K); a characteristic *wnt11*$^{-}$ phenotype revealing defective organizer function due to disrupted prechordal plate morphogenesis (Marlow et al., 1998).

Strikingly, a substantially more severe phenotype arises when function of both Tbx16 and Wnt11 are lost in the same embryo than when the function of each is lost separately. At the same early gastrula stage when anterior advance of the prechordal domain can readily be appreciated with loss of either function singly, losing both Tbx16 and Wnt11 results in a wide *gsc* expression domain positioned just at the margin, resembling the early expression pattern we see prior to coalescence in the wild type (Fig. 4D, compare with Fig. 1B). By the end of gastrulation, in *tbx16*$^{-}$; *wnt11*$^{-}$ embryos, we observe a significant gap between the *gsc* expression domain and the anterior edge of the neural plate (marked by expression of *dlx3b*), indicating that the prechordal plate is posteriorly mispositioned in the double mutants (Fig. 4H). *gsc* expression appears as two strongly stained lateral domains with weak expression in the midline (Fig. 4H), rather than as the singular midline domain observed in wild types and the single mutants (Fig. 4E–G). We suggest that the weak midline expression means that the early coalescence movements had almost completely failed, resulting in two, largely separate fields of *gsc* expressing cells throughout gastrulation, an interpretation supported by time-lapse analysis (Movie 4).

Furthermore, in the 24 hpf *tbx16*$^{-}$; *wnt11*$^{-}$ double mutant, there is a dramatic enhancement of the *wnt11*$^{-}$ single mutant eye field separation defect (Fig. 4L; also see quantification in Supporting Fig. 2), revealing a previously uncharacterized role of Tbx16 in eye field separation. A function of Tbx16 in head mesoderm morphogenesis following coalescence seems unlikely because the pattern of *gsc* expression in *tbx16* mutants recovers to that of wild type at the end of gastrulation. Our collective data set suggests that the role of Tbx16 in organizing the organizer is in fact the regulation of Papc-mediated coalesence at gastrulation onset.

In this study, we sought to understand how the organizer region of the zebrafish embryo arises morphogenetically. We show that deep cells within the organizer, the presumptive prechordal plate cells, become a singular field after initially being composed of two domains, and that Tbx16 and its genetic target, Papc, are necessary for this to occur properly. We call the merging process coalescence and show that coalescence depends on the combined activity of Tbx16 and Wnt11. Biochemical studies have recently demonstrated that Xpapc and the Wnt receptor, Fz, physically interact and signal through common downstream effectors (Medina et al., 2004). Therefore, by blocking the function of Tbx16, Papc, and Wnt11 in the zebrafish presumptive prechordal plate, we may disrupt signalling through a conserved set of morphogenetically critical downstream effectors. Alternatively, Tbx16, Papc, and Wnt11 may signal in parallel through distinct downstream targets. Future studies will be needed to distinguish between these two possibilities. This recent work also showed that the combined loss of Xpapc and Fz leads to a dramatic failure of explanted *X. laevis* tissue to undergo cell intercalation, behaviour which is necessary for proper elongation of the notochord (Medina et al., 2004; Unterseher et al., 2004). Thus, the interaction of the non-canonical Wnt pathway and Papc is critical for morphogenesis not only in the zebrafish presumptive prechordal plate, but in other developmental contexts as well.

An unresolved question in this study is how do the two distinct coalescing domains originate? It has been proposed that the Nodal signalling pathway prevents cells at the dorsal margin from taking on neural fates, thus promoting the internalization of mesendodermal precursors (Dougan et al., 2003). Are Nodal signals and the establishment of the two initially distinct prechordal plate domains somehow related? For example, might there be a Nodal inhibitor at the precise midline position (overlying the future demarcation) that initially blocks the internalization of cells at this location? Alternatively, might a source of Nodal signal emanate from cells adjacent to the midline? In this model, the prospective future mesendodermal cells positioned at the midline would receive lower levels of Nodal signal than cells closer to the laterally positioned source, and hence would be the least likely to internalize (because Nodal is thought to promote internalization.) The presence of a source of Nodal signal on either side

of the midline is supported by the observation that in mutants with reduced Nodal activity, *gsc* expression, which is dependent on Nodal signals, is often observed as two distinct, weakly expressing domains adjacent to the midline at a time when mesendodermal cells are beginning to internalize, unlike wild type in which *gsc* is expressed as a solid midline domain (Dougan et al., 2003). Testing the validity of these two models will be an exciting future challenge.

Experimental Procedures

Staging

Early gastrulation embryos were staged as follows: embryos at the sphere to dome (S-D) transition (Kimmel et al., 1995) were isolated and used for experiments at set time points after the transition. Thus, the notation, S-D 0:45, indicates 45 minutes after the sphere to dome transition, for example. We include corresponding percent epiboly stages from (Kimmel et al., 1995) for reference; however, because these standard stages represent windows of developmental time lasting several minutes, rather than discrete time points in development, different S-D times can fall within a single standard epiboly classification.

Recordings and 4D Analysis

Recordings were made as previously described (Glickman et al., 2003) with the exception that we used a Zeiss LSM Pascal confocal microscope. We tracked cells in an *h2a*-GFP transgenic strain which allowed us to readily distinguish adjacent cells by the nuclear GFP expression. We also tracked cells using FM4-64 labeled embryos. Tracks were made with the polyline tool in Zeiss LSM Image Browser software.

Membrane labelling using FM4-64

Membranes were labeled using FM4-64 (Molecular Probes, Eugene, OR). For recordings, FM4-64 was diluted (1ug/uL) in DMSO. Approximately 20 minutes prior to imaging, FM4-64 was injected into the animal pole with special care being taken not to inject into the yolk but also to enter the enveloping layer (EVL). FM4-64 diffused rapidly throughout the embryo and remained predominantly membrane-localized for approximately 3 hours following injection. After this period, staining was observed primarily as punctate dots within the cell; these are likely internalized vesicles.

Morpholino and mRNA injections

To facilitate time-lapse analysis of embryos lacking Tbx16, we used morpholino antisense oligonucleotides (MOs) which, in our hands, completely abolish expression of Tbx16 antigen when viewed in whole mount immunocytochemistry. Tbx16-MO was injected as previously described (Tribulo et al., 2003). *wnt11*-MO sequence was 5′-ACTCCAGTGAAGTTTTTCCACAACG-3′. *dn-papc* mRNA injection were performed as previously reported (Yamamoto et al., 1998), using the following RNA concentrations [50 pg/embryo=(lo); 250 pg/embryo=(hi)].

In situ hybridization and antibody staining

in situ hybridization and Ntl antibody staining was performed as previously described (Amacher et al., 2002).

Supplementary Material

Refer to Web version on PubMed Central for supplementary material.

Acknowledgements

We would like to thank Marnie Halpern and Gage Crump for transgenic zebrafish lines and Carl-Philipp Heisenberg for constructs. We wish to express our sincerest thanks to Gage Crump, Judith Eisen and Bruce Bowerman for valuable comments during the preparation of this manuscript. John Dowd provided expert animal care. JBM was supported by an NIH Developmental Biology Training Grant (5T32HD07348). The research was funded by NIH Grant HD22486.

Reference List

Amacher SL, Draper BW, Summers BR, Kimmel CB. The zebrafish T-box genes no tail and spadetail are required for development of trunk and tail mesoderm and medial floor plate. Development 2002;129:3311–3323. [PubMed: 12091302]

Dougan ST, Warga RM, Kane DA, Schier AF, Talbot WS. The role of the zebrafish nodal-related genes squint and cyclops in patterning of mesendoderm. Development 130:1837–1851. [PubMed: 12642489]

Essner JJ, Branford WW, Zhang J, Yost HJ. Mesendoderm and left-right brain, heart and gut development are differentially regulated by pitx2 isoforms. Development 2000;127:1081–1093. [PubMed: 10662647]

Glickman NS, Kimmel CB, Jones MA, Adams RJ. Shaping the zebrafish notochord. Development 2003;130:873–887. [PubMed: 12538515]

Griffin KJ, Amacher SL, Kimmel CB, Kimelman D. Molecular identification of spadetail: regulation of zebrafish trunk and tail mesoderm formation by T-box genes. Development 1998;125:3379–3388. [PubMed: 9693141]

Gumbiner BM. Regulation of cadherin-mediated adhesion in morphogenesis. Nat Rev Mol Cell Biol 2005;6:622–634. [PubMed: 16025097]

Heisenberg CP, Tada M, Rauch GJ, Saude L, Concha ML, Geisler R, Stemple DL, Smith JC, Wilson SW. Silberblick/Wnt11 mediates convergent extension movements during zebrafish gastrulation. Nature 2000;405:76–81. [PubMed: 10811221]

Hukriede NA, Tsang TE, Habas R, Khoo PL, Steiner K, Weeks DL, Tam PP, Dawid IB. Conserved requirement of Lim1 function for cell movements during gastrulation. Dev Cell 2003;4:83–94. [PubMed: 12530965]

Kim SH, Yamamoto A, Bouwmeester T, Agius E, Robertis EM. The role of paraxial protocadherin in selective adhesion and cell movements of the mesoderm during Xenopus gastrulation. Development 1998;125:4681–4690. [PubMed: 9806917]

Kimmel CB, Ballard WW, Kimmel SR, Ullmann B, Schilling TF. Stages of embryonic development of the zebrafish. Dev Dyn 1995;203:253–310. [PubMed: 8589427]

Marlow F, Zwartkruis F, Malicki J, Neuhauss SC, Abbas L, Weaver M, Driever W, Solnica-Krezel L. Functional interactions of genes mediating convergent extension, knypek and trilobite, during the partitioning of the eye primordium in zebrafish. Dev Biol 1998;203:382–399. [PubMed: 9808788]

Medina A, Swain RK, Kuerner KM, Steinbeisser H. Xenopus paraxial protocadherin has signaling functions and is involved in tissue separation. Embo J 2004;23:3249–3258. [PubMed: 15272309]

Solnica-Krezel L. Conserved patterns of cell movements during vertebrate gastrulation. Curr Biol 2005;15:R213–228. [PubMed: 15797016]

Spemann, HaMH. Uber induction von embryonalanlagen durch implantation artfrender organisatoren. Wilh Roux Arch Entw Mech Org 1924;100:599–638.

Tribulo C, Aybar MJ, Nguyen VH, Mullins MC, Mayor R. Regulation of Msx genes by a Bmp gradient is essential for neural crest specification. Development 2003;130:6441–6452. [PubMed: 14627721]

Ulrich F, Concha ML, Heid PJ, Voss E, Witzel S, Roehl H, Tada M, Wilson SW, Adams RJ, Soll DR, Heisenberg CP. Slb/Wnt11 controls hypoblast cell migration and morphogenesis at the onset of zebrafish gastrulation. Development 2003;130:5375–5384. [PubMed: 13129848]

Ulrich F, Krieg M, Schotz EM, Link V, Castanon I, Schnabel V, Taubenberger A, Mueller D, Puech PH, Heisenberg CP. Wnt11 functions in gastrulation by controlling cell cohesion through Rab5c and E-cadherin. Dev Cell 2005;9:555–564. [PubMed: 16198297]

Unterseher F, Hefele JA, Giehl K, De Robertis EM, Wedlich D, Schambony A. Paraxial protocadherin coordinates cell polarity during convergent extension via Rho A and JNK. Embo J 2004;23:3259–3269. [PubMed: 15297873]

Warga RM, Nusslein-Volhard C. spadetail-dependent cell compaction of the dorsal zebrafish blastula. Dev Biol 1998;203:116–121. [PubMed: 9806777]

Yamamoto A, Amacher SL, Kim SH, Geissert D, Kimmel CB, De Robertis EM. Zebrafish paraxial protocadherin is a downstream target of spadetail involved in morphogenesis of gastrula mesoderm. Development 1998;125:3389–3397. [PubMed: 9693142]

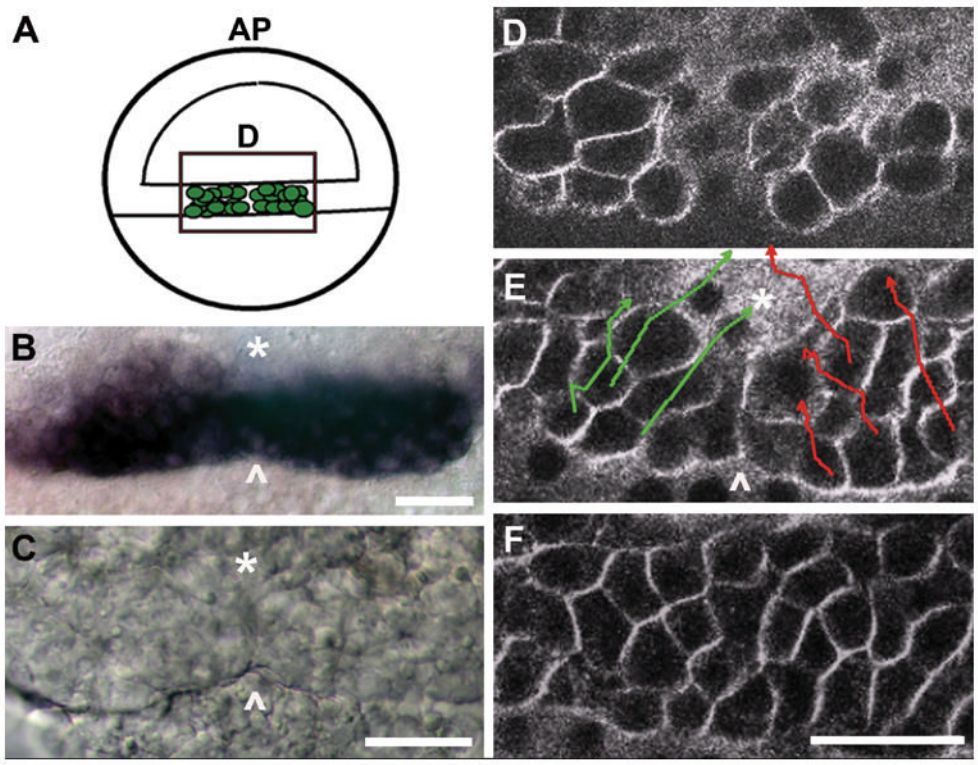

Fig. 1. The early presumptive prechordal plate is initially comprised of two spatially distinct domains that merge into a singular, midline field.

(A) Schematic of the embryo at gastrula onset (50% epiboly, S-D 1:15), representing the newly internalized presumptive prechordal plate, depicted as green cells within the rectangle. Images in B–D correspond to the boxed region represented in the schematic. Green, presumptive prechordal plate cells are located within the germ ring. Blastoderm is located on the top half of the schematized 50% epiboly embryo. AP: animal pole. D: dorsal.

(B) *gsc* expression at 45% epiboly (S-D 1:10). Arrowhead marks the position of the demarcation.

(C) Nomarski DIC image at 45% epiboly (S-D 1:10). The boundary between the initially distinct domains is represented by an asterisk and the arrowhead marks the position of the demarcation.

(D–F) Cells at the dorsal margin were tracked for a period of one hour, from just prior to 40% epiboly (S-D 0:45) to 55% epiboly (S-D 1:50) using FM-4-64 which labels cell membranes making it possible to distinguish individual cells. Image in D shows the first frame of the recording, with newly internalized cells forming two separate inward bulges into the yolk syncitial layer. Tracks in E represent trajectories of individual cells over the 65 minute period. The end time point of each track is represented by an arrow. Image in E represents the 30 minute time point when the demarcation is evident (indicated with an arrowhead. F shows the final frame of the recording at which time the demarcation is erased. *flh*-GFP expression is enhanced at the dorsal margin and was used to mount embryos dorsally prior to the appearance of the shield. The asterisk marks the position of the dorsal midline. Arrowhead marks the position of the demarcation. Scale bars: 50 μm.

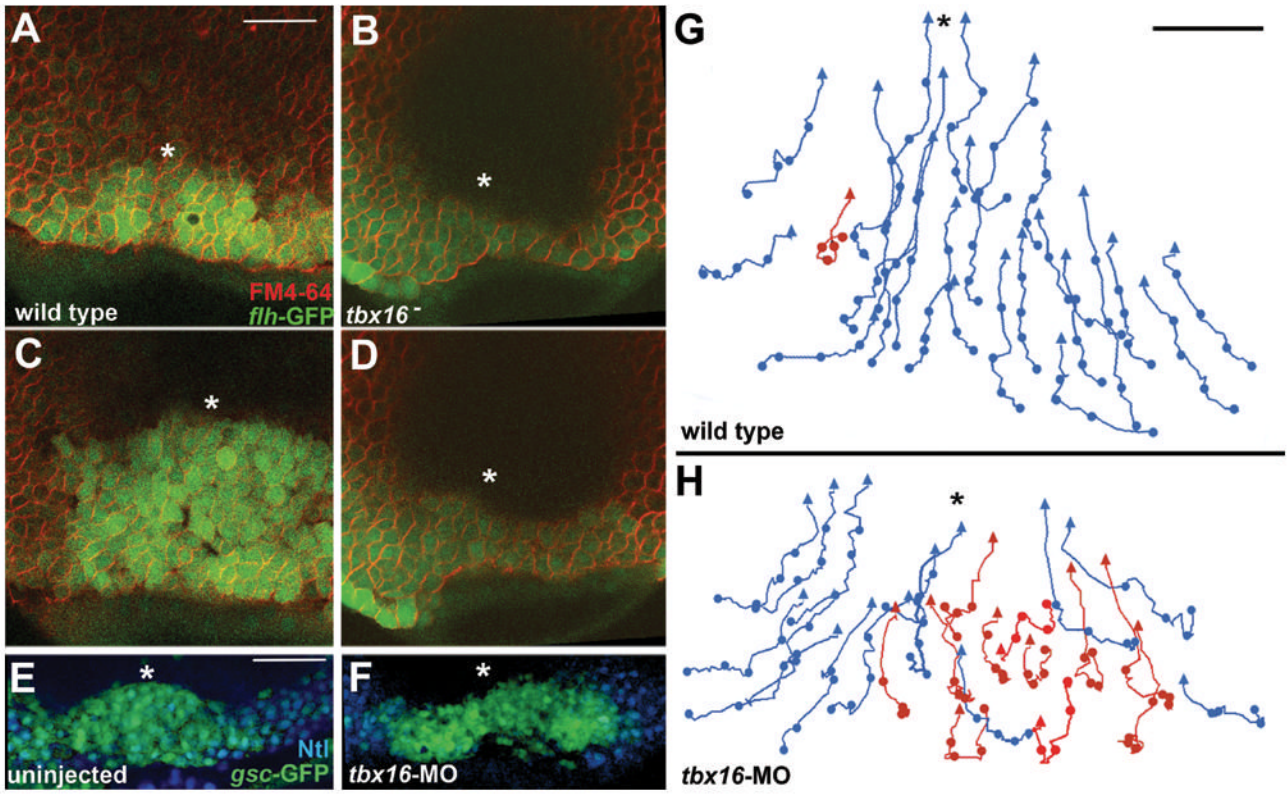

Fig. 2. Presumptive prechordal plate coalescence is disrupted in *tbx16* mutants and *tbx16*-MO embryos.

(A–D) Recordings of movements of the presumptive prechordal plate were made starting at S-D 1:15. *flh*-GFP marks internalized cells at the midline. (A) Wild-type embryo is shown at time 0:00. Note that unlike endogenous *flh* expression, *flh*-GFP is expressed in both presumptive prechordal plate and notochord cells at these timepoints. FM4-64 was used to label the membranes of cells. The asterisk indicates the position of the midline. Dorsal view with animal pole up (A–H).

(B) Panel shows a *tbx16*$^{-}$ embryo at time 0:00. *tbx16*$^{(b104)}$ was used in all experiments. We observed a similar phenotype in *tbx16*-MO embryos.

(C) Panel shows the same wild-type embryo as in A at time 30:00.

(D) Panel shows the same *tbx16*$^{-}$ embryo as in B at time 30:00.

(E–F) Confocal section of a wild type embryo fixed shortly after the initiation of anterior presumptive prechordal plate translocation (S-D 1:25). Presumptive prechordal plate cells in (E) an uninjected embryo and (F) a *tbx16*-MO embryo were labeled with *gsc*-GFP (green) and Ntl expression (blue) visible in marginal cells adjacent to the presumptive prechordal plate.

(G–H) Shows tracks of cell movements during a 60 minute recording. Recording starts at 50% epiboly. Midline is represented with an asterisk. Tracks of an uninjected embryo (G) and a *tbx16*-MO embryo (H). Tracks displaying directed movement are color-coded blue and tracks displaying aberrant movement are color-coded red. Scale bar represents 100um in (A–F) and 50um in (G–H).

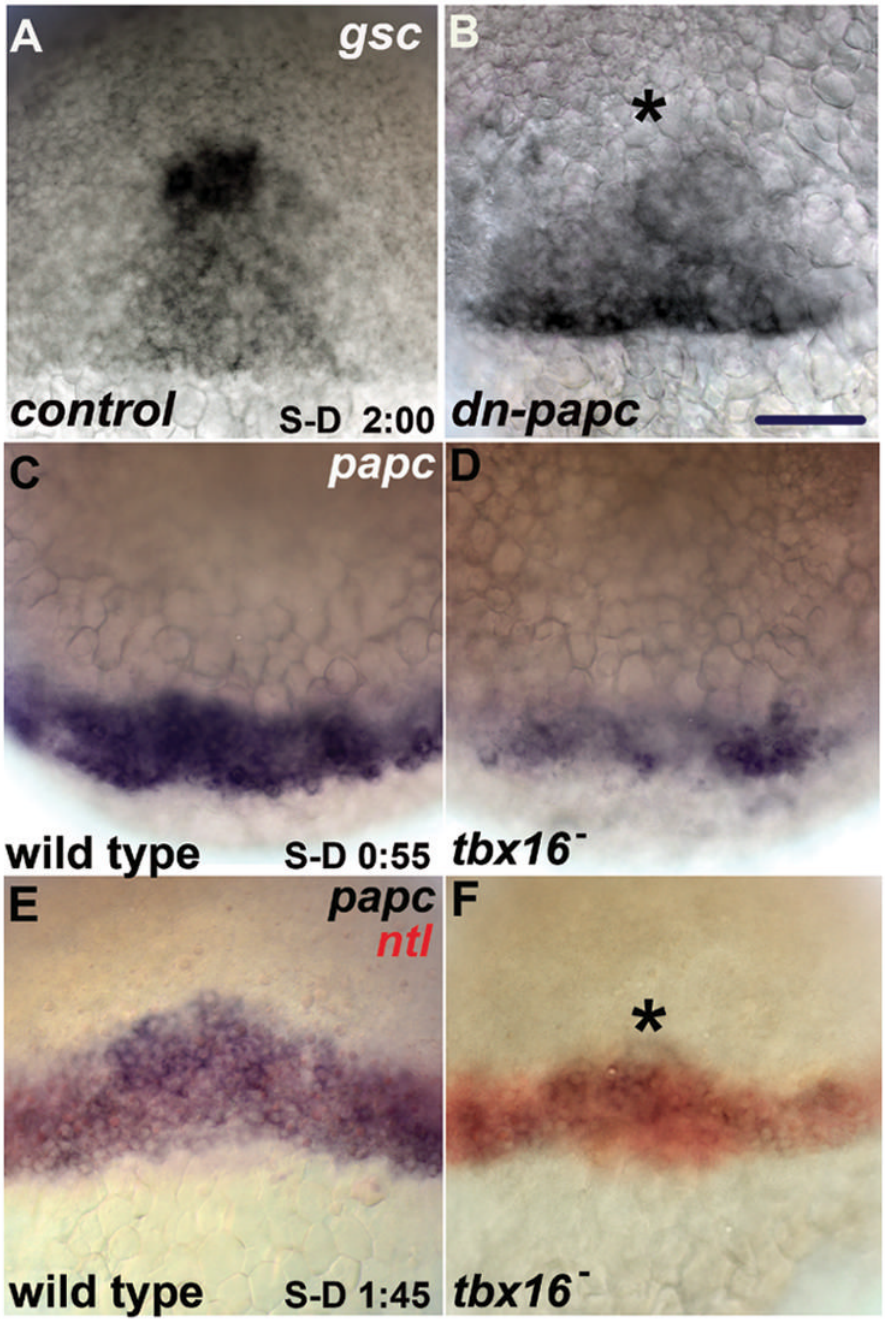

Fig. 3. Blocking Papc function disrupts presumptive prechordal plate marker expression, and Papc is expressed in patches in the coalescing presumptive prechordal plate in *tbx16* mutants.

(A–B) *gsc* expression at early-mid gastrulation (S-D + 2:10) in a (A) control embryo (*cytoplasmic-gfp* mRNA injected) and a (B) *dn-papc* mRNA (lo) embryo . Animal pole is up and dorsal view is shown in (A–F). Asterisk marks position of midline in (A–F). (C–D) *papc* expression in late blastula (S-D + 0:55) in (C) wild type and (D) *tbx16*$^{-}$. (E–F) *papc* expression in early shield stage (S-D + 1:45) in (E) wild-type and (F) *tbx16*$^{-}$. *papc*-expressing cells in *tbx16*$^{-}$ consistently co-localize with the dorsal margin expression of *ntl (red). ntl* expression extends farther anteriorly on the dorsal aspect of the embryo, is not expressed in hypoblast

cells at this early stage, and thus we use it as a marker of dorsal in this experiment. Scale bars: 50 μm.

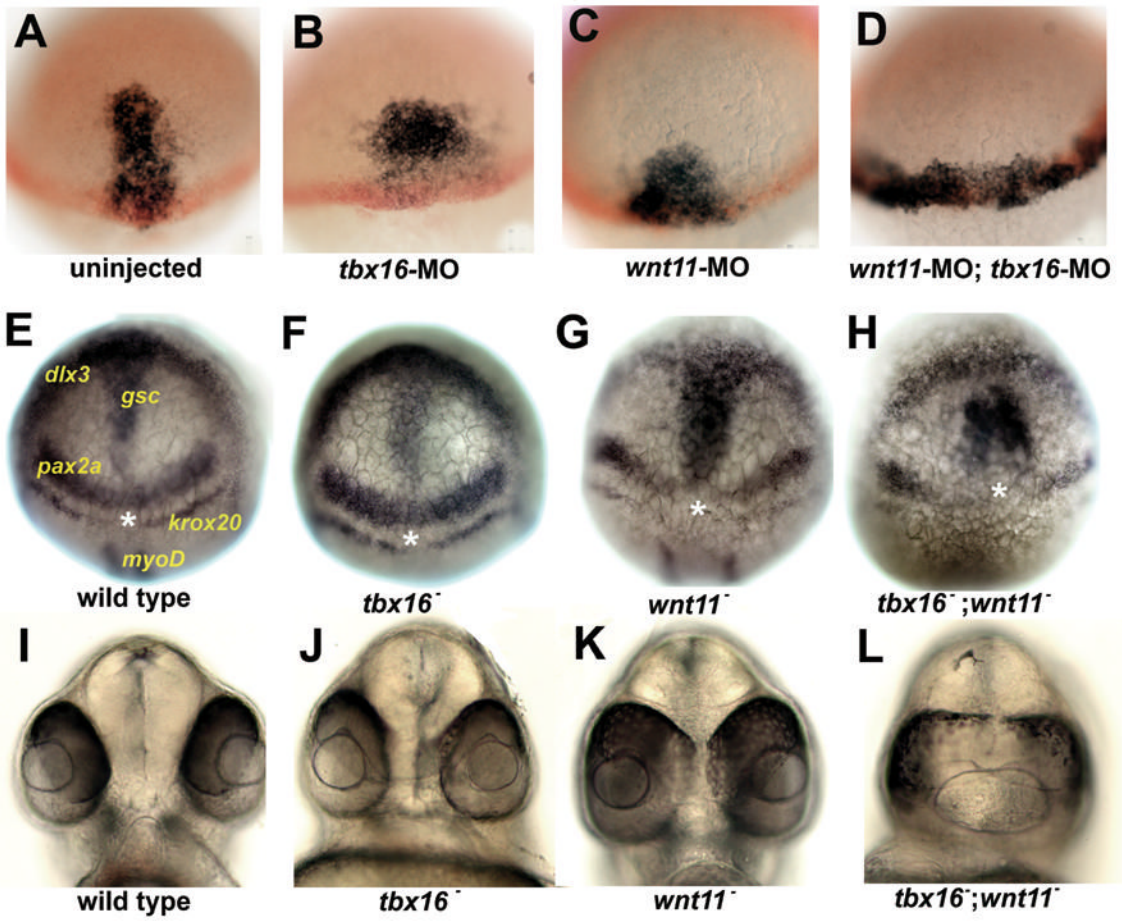

Fig. 4. Loss of Tbx16 enhances prechordal plate marker misexpression and the eye field separation defect of embryos with reduced Wnt11 function.

(A–D) Prechordal plate marker expression at early-mid gastrulation (S-D 2:10). *gsc* (black) labels presumptive prechordal plate and *ntl* (red) labels the margin. MO treatment is indicated on the panel. Dorsal view and animal pole is up in (A–H). (E–H) Prechordal plate marker expression at the end of gastrulation (bud stage). Genotypes indicated on panel. Position and identity of mRNA are indicated in E. *gsc* labels prechordal plate cells. *dlx3* labels the anterior edge of the neural plate. *pax2a* and *krox20* label the midbrain hindbrain boundary and rhombomere 3 at this stage and were used to identify *wnt11*$^{-}$ because these expression domains fail to meet at the midline in *wnt11*$^{-}$. *myoD* labels adaxial cells and was used to identify *tbx16*$^{-}$ because *tbx16*$^{-}$ has reduced *myoD* expression at bud stage. Asterisk indicates position of midline. (I–L) Panels show frontal view of the zebrafish face illustrating the degree of eye field separation in (I) wild type, (J) *wnt11*$^{-}$, (K) *tbx16* $^{-}$, and (L) *wnt11*$^{-}$; *tbx16* $^{-}$ embryos. *wnt11*^{tz216} was used in all relevant experiments. See Supporting Fig 2 for quantification.